

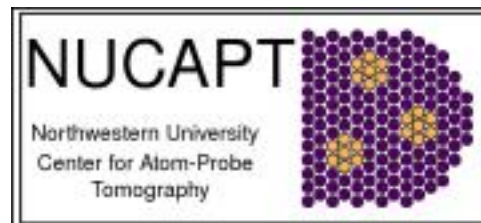
Understanding kinetics of phase transformations in precipitation-strengthened low-alloy steels and its influence on mechanical properties

Steel Research Group Meeting,
24th March, 2014, Monday
Divya Jain and David N. Seidman
Northwestern University

Department of Materials Science and Engineering
Evanston, Illinois 60208-3108



NORTHWESTERN
UNIVERSITY



Presentation Outline

- **Introduction to high-strength low-alloys (HSLA) steels used in U. S. Naval applications**
- **Development and implementation of HSLA-115: where 115 is the yield strength in ksi**
- **Mechanical properties and 3-D atom-probe tomography (APT) results for as-received HSLA-115**
- **3-D atom-probe tomography results for HSLA-115 aged at 550°C**
- **Mechanical properties of NuCu-140 steels: NuCu = Northwestern University Cu precipitation strengthened steels, where 140 is the yield strength in ksi.**

High-Strength Low-Alloy (HSLA) Precipitation Strengthened Steels: Naval Applications

HY (High Yield)

Carbon content
0.12-0.20 wt.%

Microstructure in heat-affected zone (HAZ) susceptible to hydrogen-induced cracking

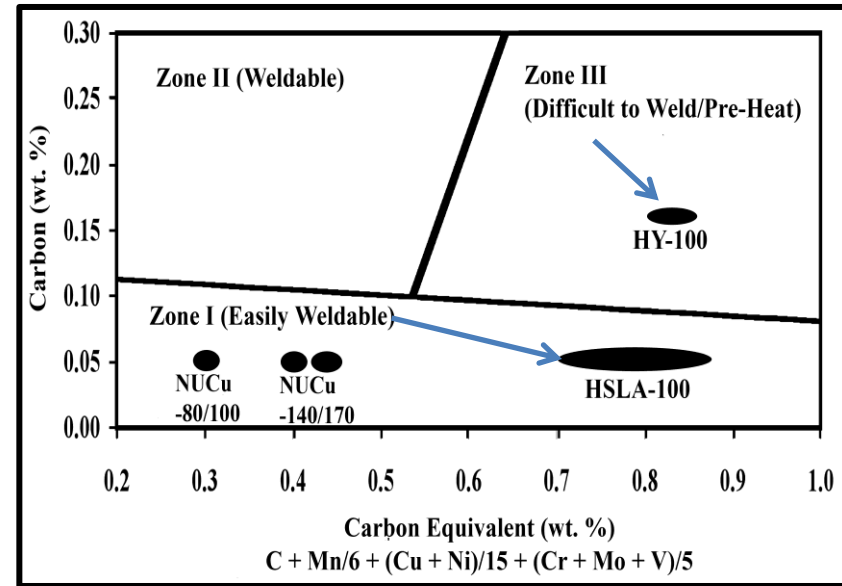
High degree of preheat, post-weld heating, and stringent control requirements on welding processes increases processing costs

HSLA-100

Carbon content
<0.06 wt.%

Low-carbon concentration enhances weldability, but limits the strength

Cu addition is for precipitation strengthening provided by nanosize Cu-precipitates



Graville Diagram¹

Development and Implementation of HSLA-115

- **Modified version of HSLA-100: Composition-3**
- **Objective is to increase the yield strength and concomitantly meet other property requirements**
- **Higher strength results in weight reduction and increases factor of safety for critical applications, where thickness reduction is not desired.**
- **Approved for plate production in January 2009; currently used for the flight deck of USS Gerald R. Ford carrier, CVN 78**
- **Development has been mostly empirical; no detailed investigations to date**

HSLA-100 (Comp-3)

Element	Comp (wt%)
C	0.06 max
Cu	1.15-1.75
Ni	3.35-3.65
Al	0.015 min
Mn	0.75-1.15
Si	0.40 max
Cr	0.45-0.75
Mo	0.55-0.65
Nb	0.02-0.06
P	0.02 max
S	0.004max



USS Gerald R. Ford (CVN 78)

Design Chemistry of HSLA-115

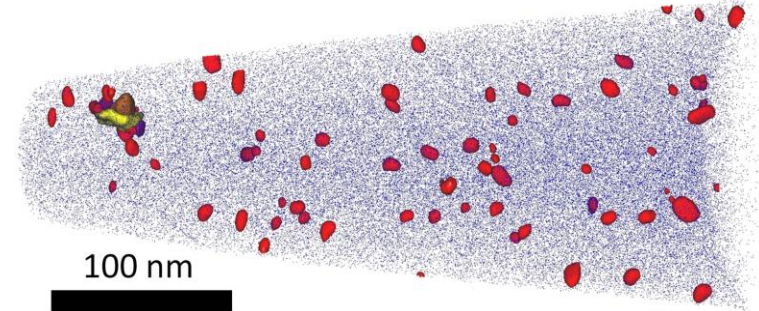
- **Carbon** concentration is small to limit the preheating requirements during welding.
- **Copper** precipitation strengthening is utilized to meet the strength requirements.
- Alloying additions of **Cr and Mo** are for increasing hardenability, so that a lath martensitic/bainitic microstructure results on quenching.
- Microalloying additions of **Nb** are for refining the grain size during high-temperature rolling and solutionizing treatments
- **Nickel** addition improves the low-temperature impact toughness and prevents hot shortness that can result due to Cu-addition.
- **Mn** addition getters sulphur impurities, and provides solid-solution strengthening along with **Si**.

HSLA-100 (Comp-3)

Element	Comp (wt%)
C	0.06 max
Cu	1.15-1.75
Ni	3.35-3.65
Al	0.015 min
Mn	0.75-1.15
Si	0.40 max
Cr	0.45-0.75
Mo	0.55-0.65
Nb	0.02-0.06
P	0.02 max
S	0.004max

As-Received HSLA-115 from NSWC Carderock Division

- **Heat Treatment**
Solution-treated at 913°C by “double-austenitization” treatment and water quenched. Aged at 660°C for 49 minutes and air cooled.
- **3-D Atom-probe tomographic (APT) observations.**
 - Over-aged Cu precipitates,
 $\langle R \rangle = 4.36 \pm 2.05 \text{ nm}$
 $N_v = 2.0 \pm 0.5 \times 10^{22} \text{ m}^{-3}$
 - M_2C precipitates were rarely observed
- Motivation to temper at 550°C
 - Suitable tempering temperature to facilitate precipitation of M_2C (M = Mo, Cr, Fe) metal carbides along with Cu-precipitates



3-D APT reconstruction of as-received HSLA-115¹

Mechanical Properties of as-received HSLA-115

Yield strength (YS)	806.23±9.55 (MPa)
	116.93±1.38 (ksi)
Elongation to failure (%)	23.32±0.15
Impact Toughness	139.67±16.50 ft-lbs (-84.4°C)
	164.67±10.26 ft-lbs (-18°C)

Characterization of the nanostructure of HSLA-115 aged at 550°C using 3-D atom-probe tomography

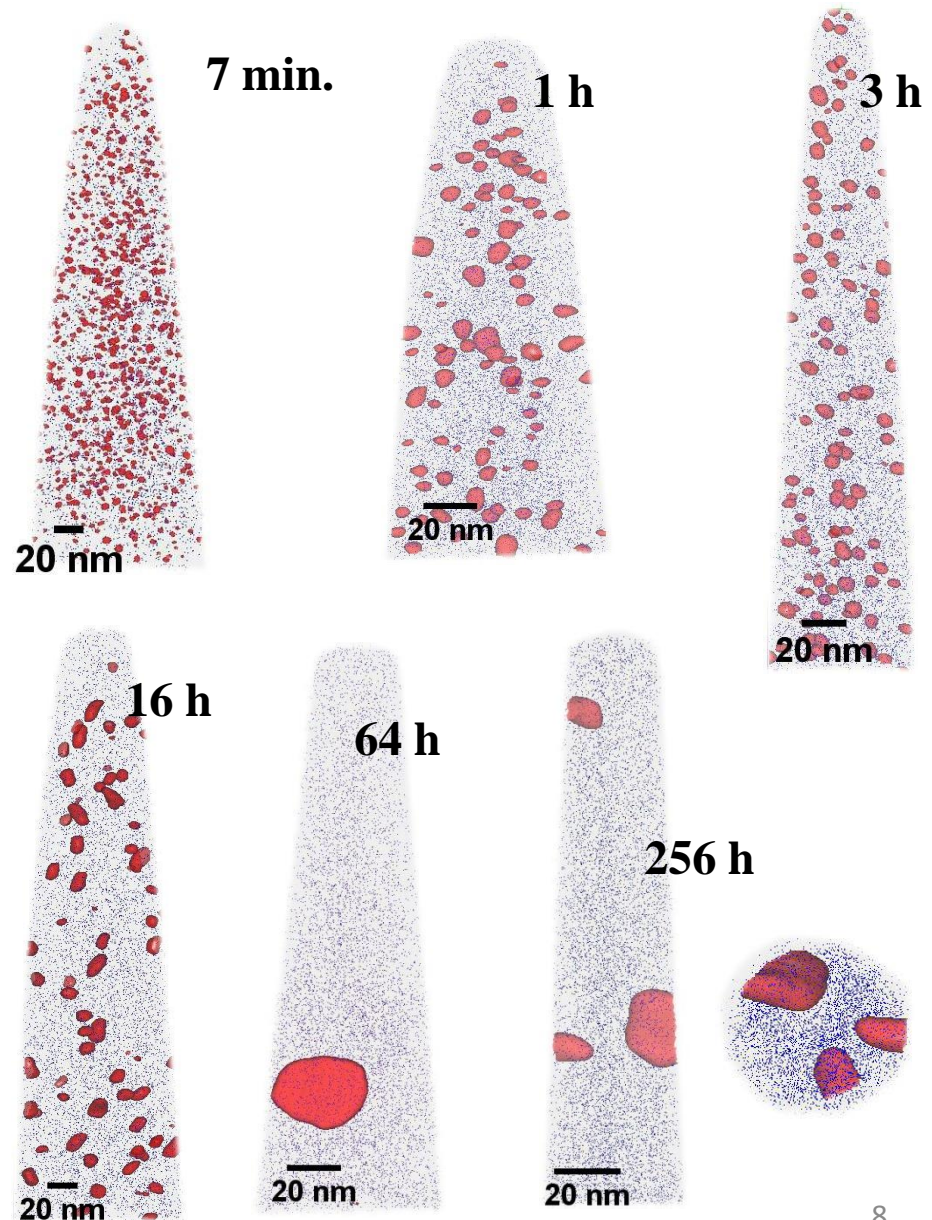
Aging study from 7 minutes to 256 h

- **Temporal evolution of copper precipitates at 550°C**
- **Temporal evolution of M_2C carbides at 550°C**
- **Niobium carbide precipitates observed in solutionized and as-quenched sample, and 16 h aged samples**
- **Coarse-cementite precipitates observed at 0.25 h of aging**
- **Colocated Cu precipitates and M_2C carbides observed at intermediate aging times of 0.25, 1, 3 and 16 h**

Temporal evolution of Cu-precipitates at 550°C

Cu precipitates are delineated by Cu-10 at. % iso-concentration surfaces (shown in red). Matrix Fe-atoms are shown in blue (only a fraction is displayed for clarity)

- Cu-precipitates were *not* observed in the solutionized and as-quenched HSLA-115.
- Profuse Cu-precipitation occurs *after 7 minutes of aging*.
- Cu-precipitates transform from spherical precipitates to ellipsoids, discs and rod-morphologies with increasing aging time



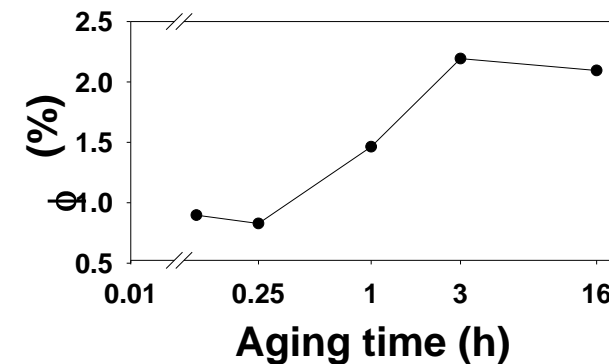
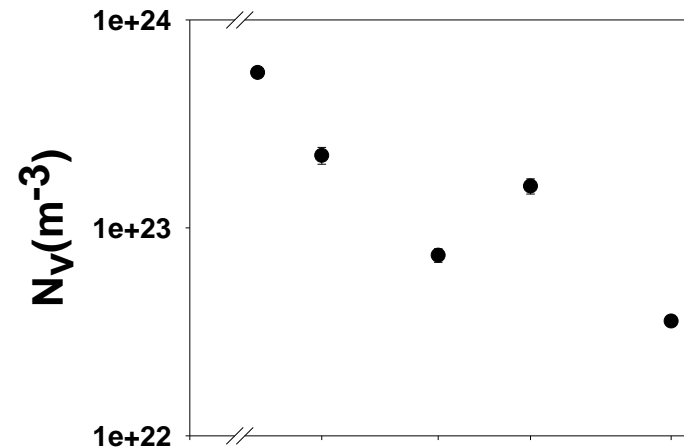
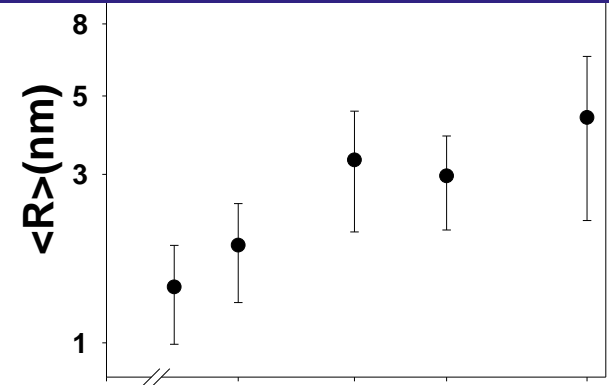
Temporal evolution of Cu-precipitates at 550°C

$\langle R(t) \rangle$: Average radius (nm)

$\phi(t)$ %: Volume fraction

$N_v(t)$: Number density (m^{-3})

- Kinetics of Cu precipitation in HSLA-115 steel is complex.
- Evolution of Cu-precipitates is influenced by the co-located M_2C carbides at intermediate aging times, in particular from 1 h to 16 h
- $\langle R(t) \rangle$ is nearly the same at 1 and 3 h of aging, with a concomitant increase of $N_v(t)$ and $\phi(t)$ indicating nucleation regime
- M_2C carbides and dislocations can be providing a reduced driving force for nucleation of Cu-precipitates, even with a significantly reduced supersaturation during this period.

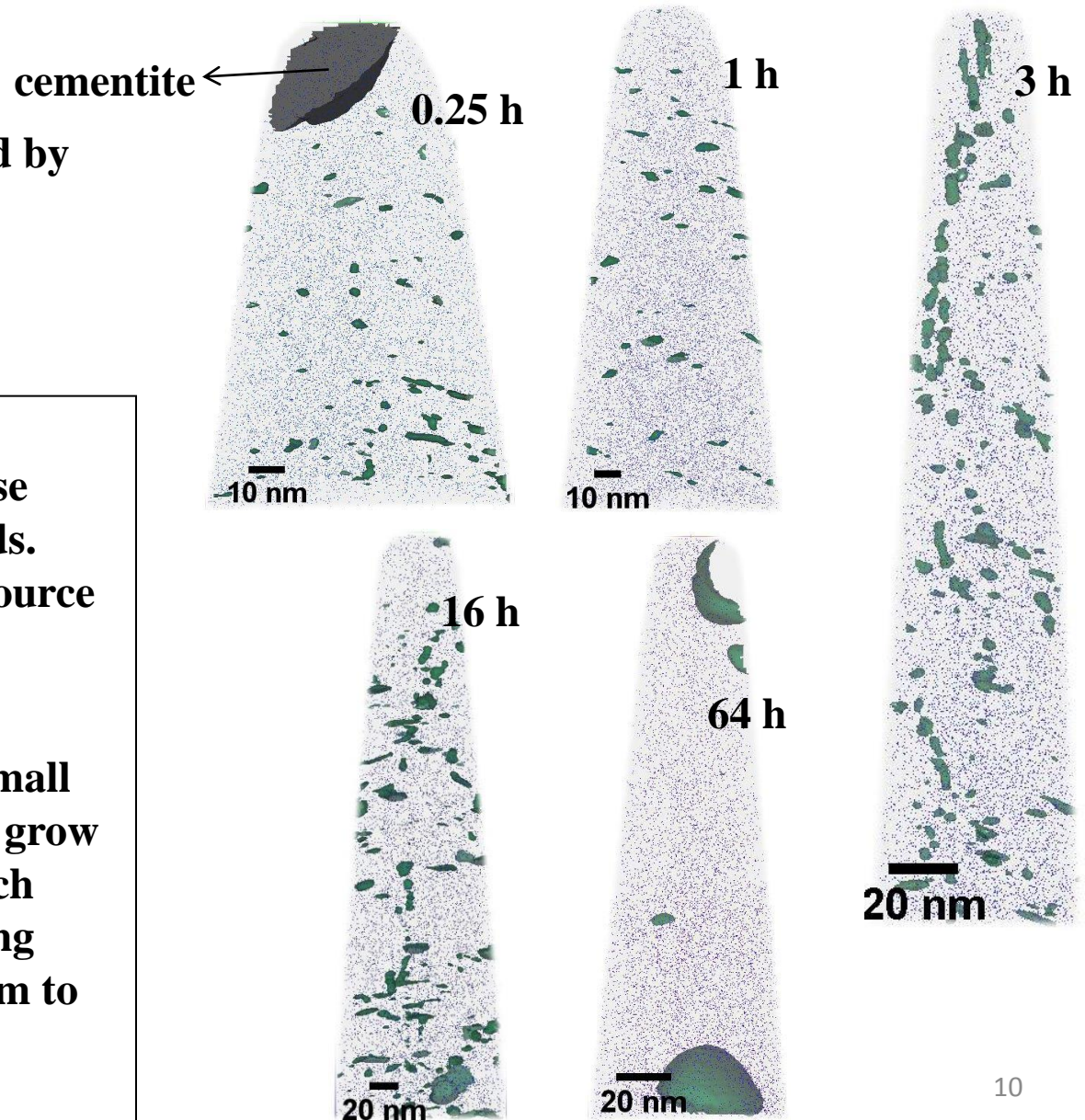


$N_v(t) > 10^{23} m^{-3}$ even after 3 h of aging

Temporal evolution of M_2C carbides at 550 °C

M_2C carbides are delineated by 5 at.% (C + Cr + Mo) iso-concentration surfaces (displayed in dark green).

- A fine dispersion of M_2C carbides replaces the coarse cementite as aging proceeds. Dissolving cementite is a source of carbon atoms for M_2C carbides.
- M_2C carbides nucleate as small spheroidal precipitates and grow as needles and/or rods, which thicken with increasing aging time. These finally transform to large irregular spheroids



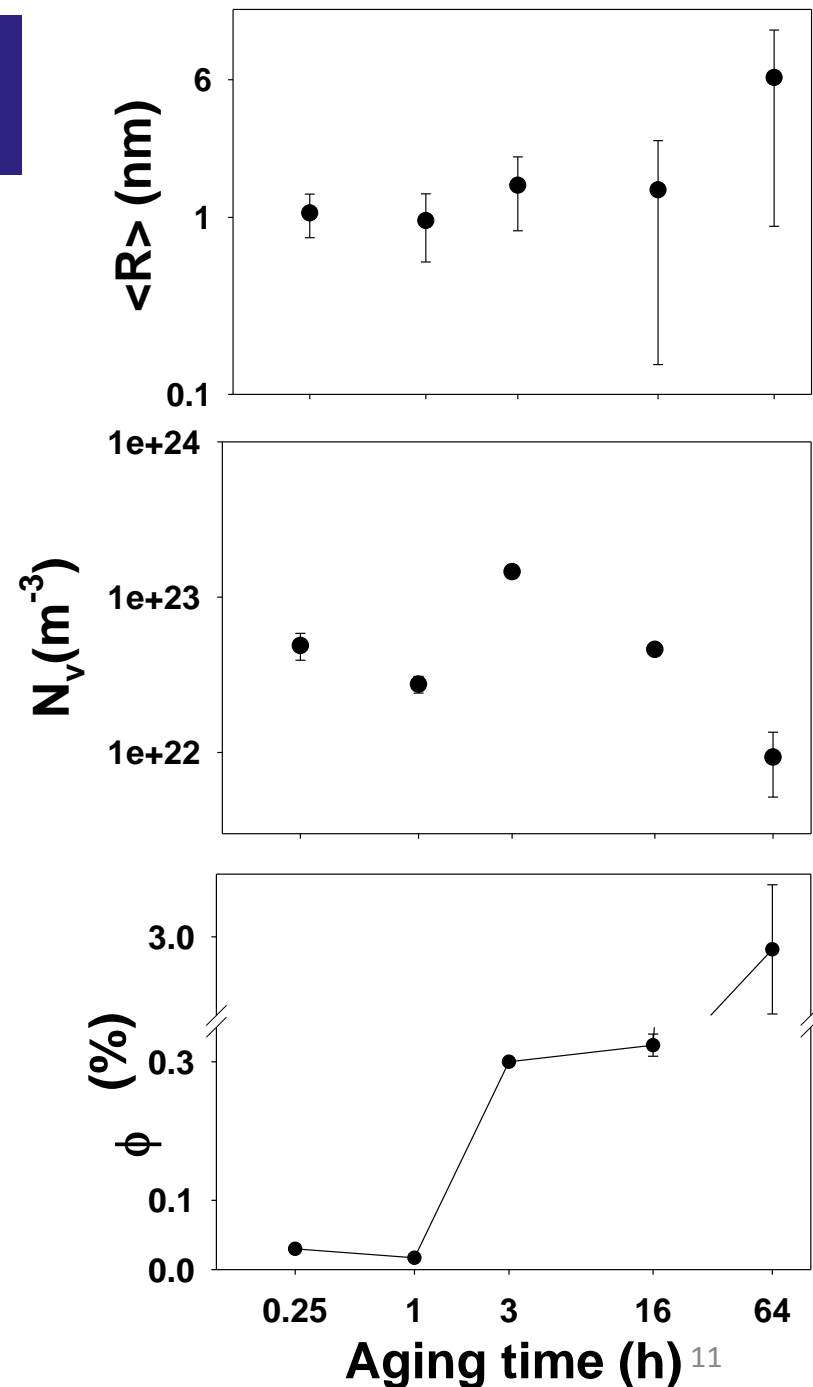
Temporal evolution of M_2C carbides at 550°C

$\langle R(t) \rangle$: Average radius

$\phi(t)(\%)$: Volume fraction

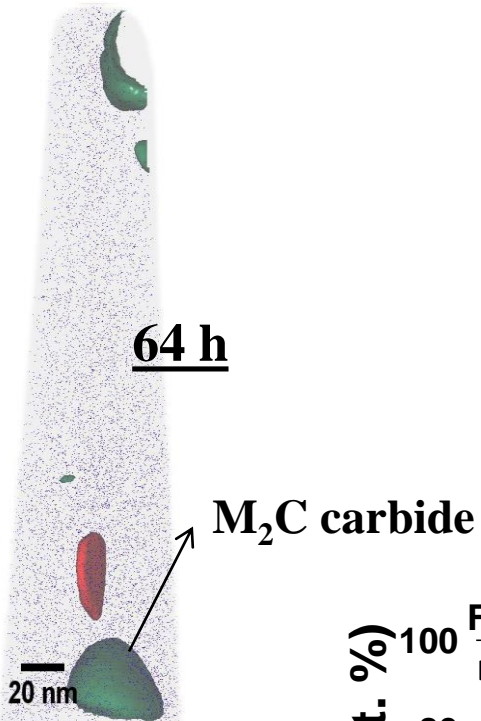
$N_v(t)$: Number density

- $\langle R(t) \rangle$ is nearly the same between 0.25 to 3 h of aging.
- $N_v(t)$ increases significantly after 1 h of aging and has a maximum at 3 h.
- $\phi(t)$ increases from 1 to 3 h. This implies nucleation occurring until 3 h of aging
- $\phi(t)$ increases significantly after 16 h with a concomitant increase in $\langle R(t) \rangle$ and decrease in $N_v(t)$, indicating the occurrence of growth and coarsening between 16 h and 64 h of aging



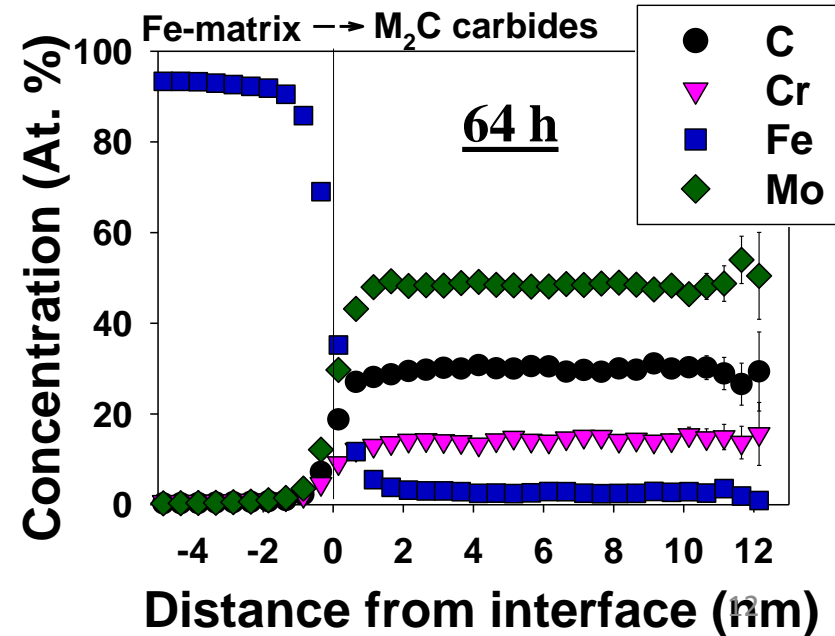
Composition of M_2C carbides: $M = Mo, Cr, Fe$

- M_2C carbides at shorter aging times (< 3 h) are enriched in Fe, depleted in C and have nearly equal Cr and Mo concentrations.
- Composition at early aging times *may be affected* by local magnification effects, arising due to differences in the evaporation fields of the M_2C carbides and the matrix, Fe atoms



At. %	Concentrations obtained from the proxigrams ($\pm 2\sigma$)
Mo	48.4 \pm 0.3
Cr	14.2 \pm 0.2
Fe	2.8 \pm 0.1
Mn	3.2 \pm 0.1
C	30.0 \pm 0.3

- At longer aging times (64 h), the Cr-to-Mo ratio as well as the Fe-concentration decreases significantly; the proxigram on the right-hand side displays the concentration profiles across the Fe/ M_2C interface at 64 h of aging

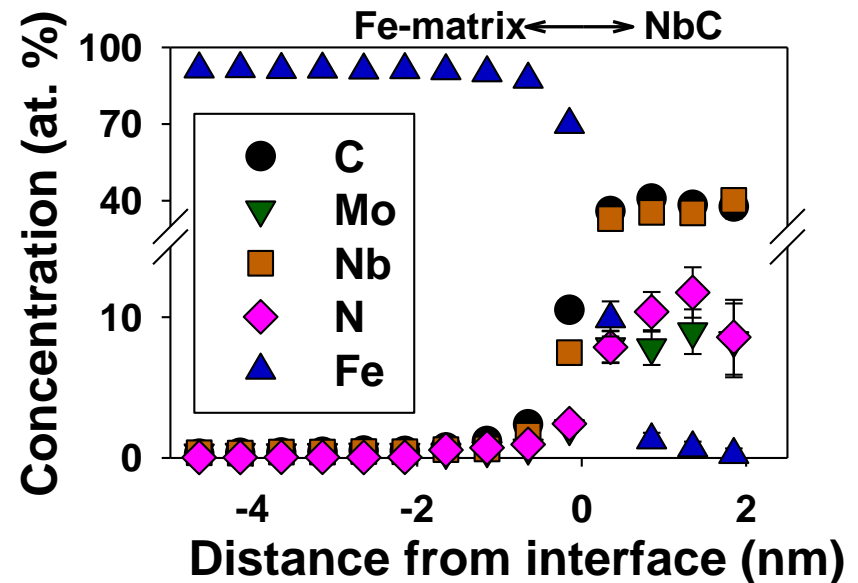
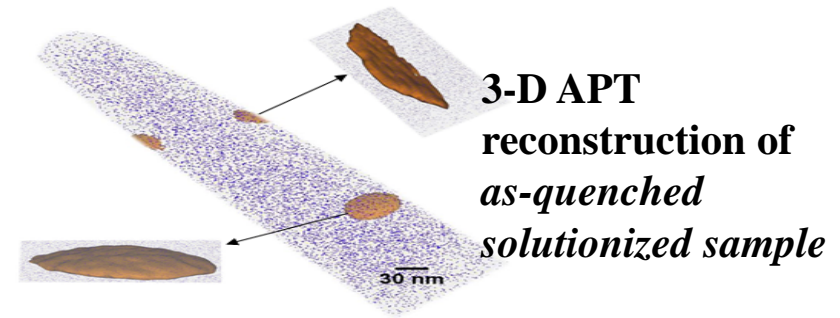


Other microstructural Observations

- **Niobium carbide precipitates are observed in solutionized and quenched sample and 16 h aged samples:**
 - Microalloying additions of Nb to HSLA steels refine the grain size.
 - Number density observed of precipitates $<10^{21} \text{ m}^{-3}$
 - Significant concentrations of nitrogen and molybdenum in these precipitates
- **A coarse cementite precipitate is observed at 0.25 h of aging:**
 - Coarse morphology of cementite is deleterious to impact toughness.
 - Enrichment of Mn, Cr and Mo and depletion of Si occurs in the cementite phase.
- **Sequence of precipitation of Cu precipitates and M_2C carbides:**
 - Cu precipitates appear first at 7 minutes of aging while M_2C carbides are not observed at this aging time
 - M_2C carbides first appear at 0.25 h of aging time. They are observed to be co-located with Cu-precipitates at intermediate aging times of 0.25, 1, 3 and 16 h

Niobium carbide precipitates observed in solutionized and as-quenched sample and 16 h aged samples

- NbC precipitates are delineated by Nb-3 at.% isoconcentration surfaces (displayed in brown).
- Cu precipitates are not observed in solutionized and as-quenched sample.
- Disc-shaped NbC precipitates are observed; they weren't dissolved during the solutionizing treatment at 912°C
- Number density observed is $<10^{21}m^{-3}$, though their detection in the 16 h aged sample suggest that these are present at all the aging times studied

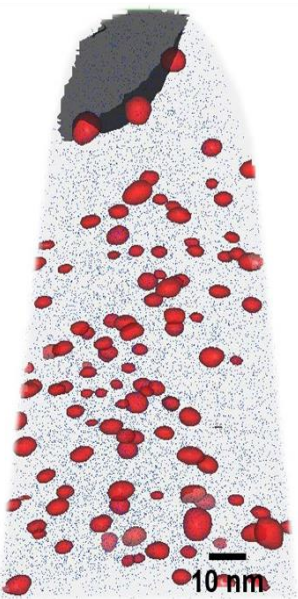


Core concentrations in niobium carbide

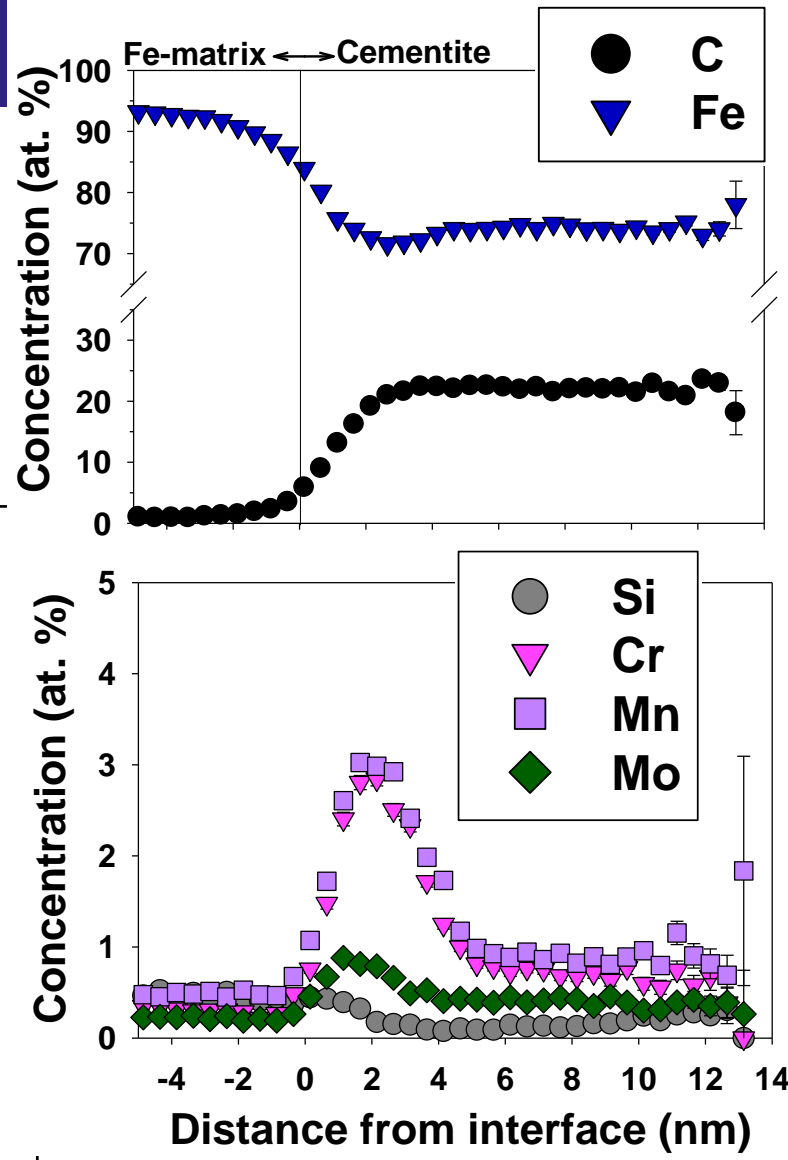
Element	Nb	Mo	C	N
At.% ($\pm 2\sigma$)	36.0 \pm 1.7	8.3 \pm 1.0	40.1 \pm 1.7	10.4 \pm 1.1

Cementite in 0.25 h aged sample

- Cementite is delineated by a C-5 at.% isoconcentration surface, shown in black in the 3-D atom-probe tomography reconstruction shown below
- To the right is displayed proxigram across the Fe/cementite interface



- There are localized concentration peaks of Mn, Cr and Mo observed near the interface on the cementite side of the precipitate
- Depletion of Si occurs in the core of the cementite precipitate.

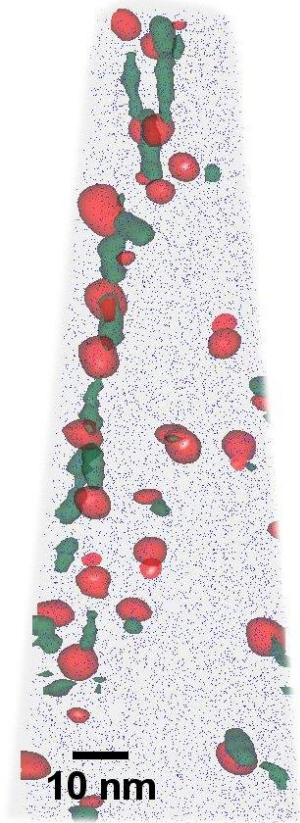
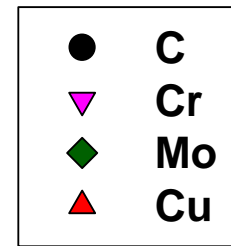


Chemical composition of the core of cementite precipitate

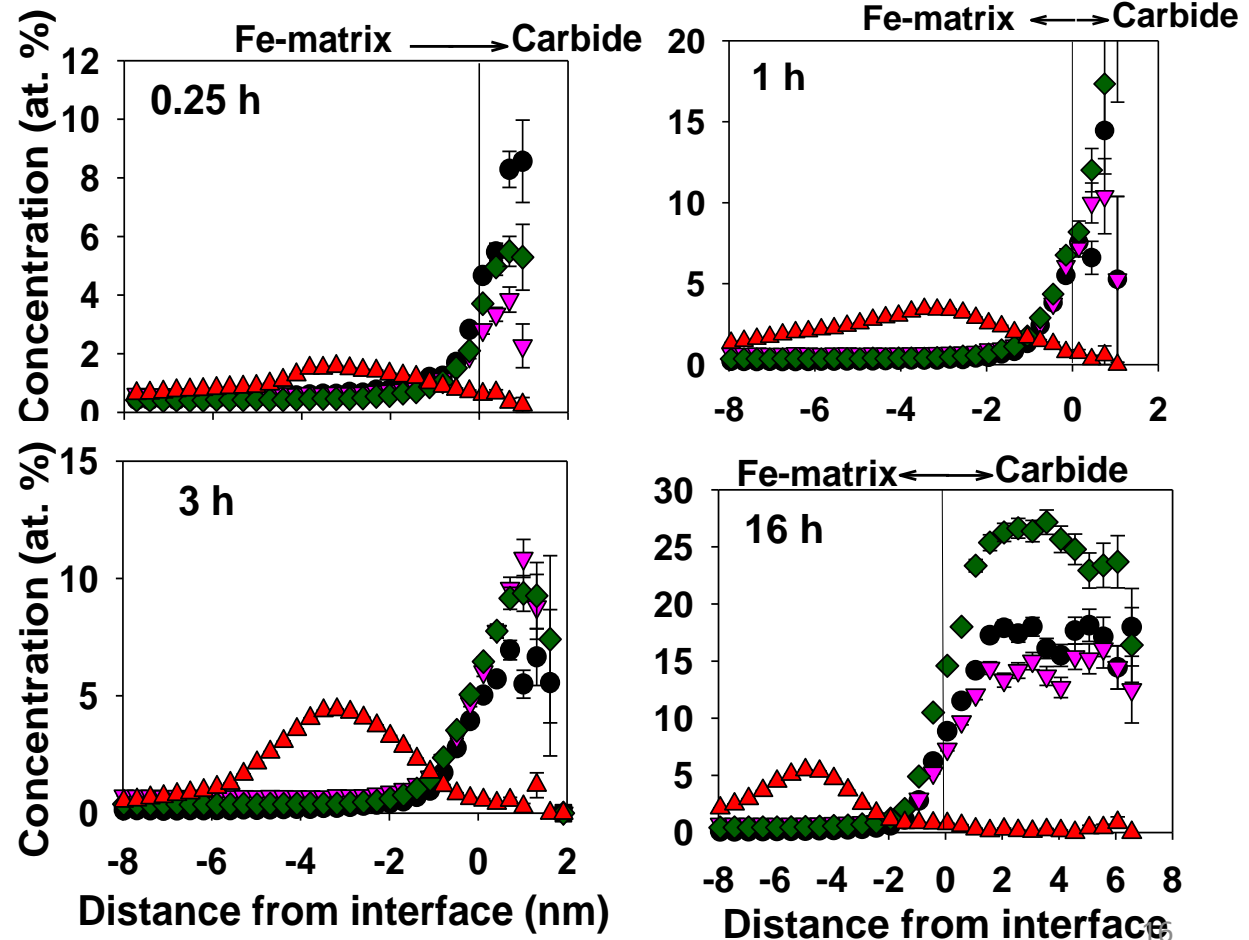
Element	Fe	C	Mo	Cr	Si	Mn	Ni
At.%(±2σ)	71.2±0.1	23.3±0.1	0.4±0.02	0.83±0.03	0.12±0.01	1.0±0.03	2.3±0.05

Co-location of Cu-precipitates and M_2C carbides

Localized enrichment in the concentration profiles of Cu near the Fe-matrix/Cu-precipitate interface, on the matrix side of the interface, indicating co-location of Cu precipitates and M_2C carbides



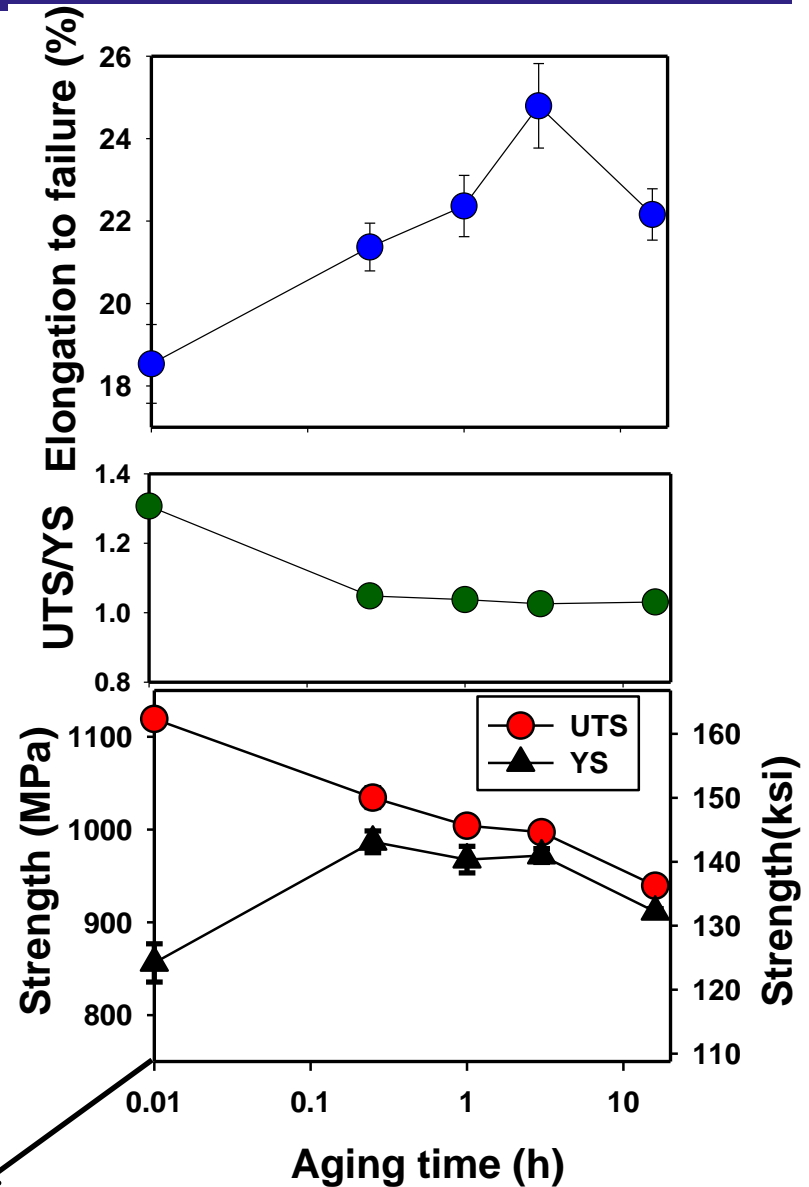
3-D atom-probe tomographic reconstruction of 3h aged sample



**Mechanical
Properties
obtained for
HSLA-115 aged at
550°C**

Trends in the tensile properties of HSLA-115

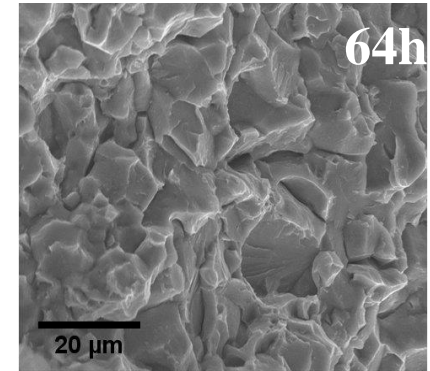
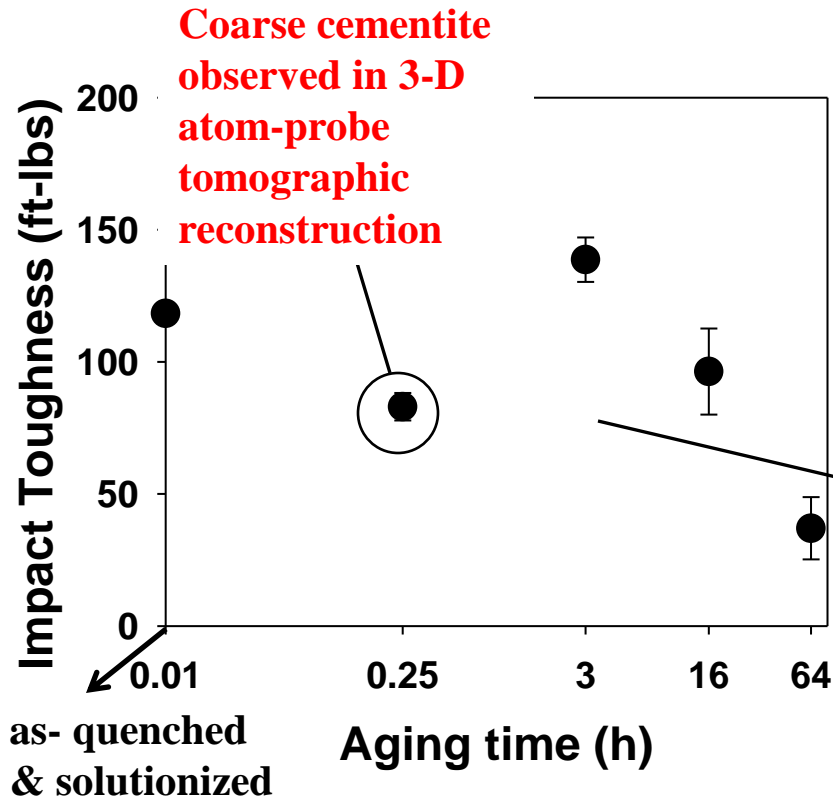
- UTS is a maximum for the solutionized and as-quenched HSLA-115, while the YS attains its maximum value at 0.25 h of aging
- Plateau region is observed for both the UTS and YS trends at intermediate aging times
- Negligible work-hardening except for the as-quenched sample
- Elongation to failure is minimum for the as-quenched sample. It increases with aging time and attains maximum at 3 h of aging



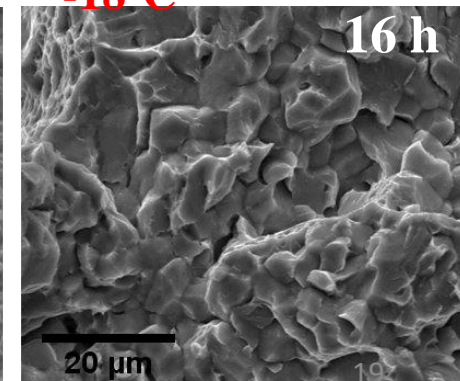
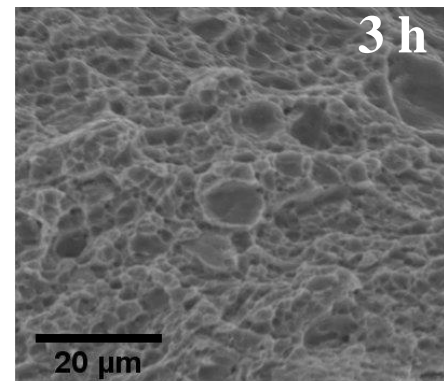
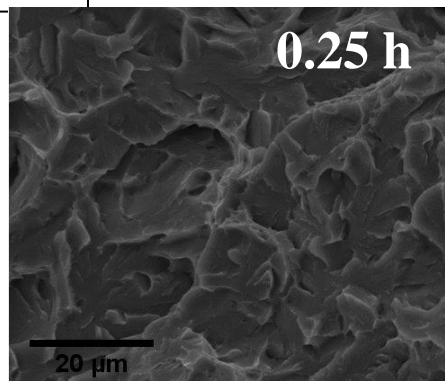
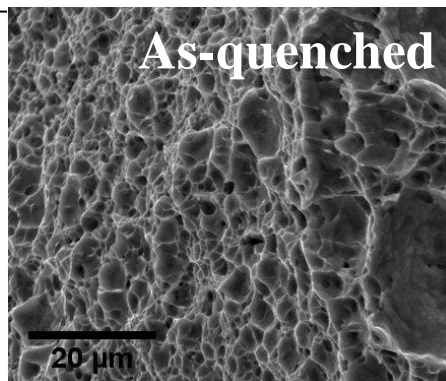
Solutionized & as- quenched

Charpy Impact Toughness at -18°C of HSLA-115

- Toughness decreases significantly after 0.25 h of aging
- Maximum toughness at 3 h
- Prolonged aging at 64 h results in minimum toughness
- SEM fractographs in qualitative agreement with obtained toughness



80 ft-lbs is the minimum impact toughness requirement of these steels for Naval applications at -18°C



Comparisons between the mechanical properties of HSLA-115 and NuCu-140 steels with sub-nanoscale microstructural information obtained using 3-D atom-probe tomography

(Both steels aged at 550°C)

Chemical Composition (wt. %)

Elements	HSLA-115	NuCu-140
C	0.05	0.05
Cu	1.29	1.64
Ni	3.37	2.77
Al	0.02	0.59
Mn	0.97	0.48
Si	0.22	0.50
Nb	0.02	0.065
<u>Cr</u>	<u>0.69</u>	<u>0.02</u>
<u>Mo</u>	<u>0.33</u>	<u>:</u>

Comparison between HSLA-115 and NuCu-140

HSLA-115

Addition of Cr & Mo increases hardenability, results in a predominantly lath martensitic/bainitic microstructure of the as-quenched sample

Aging at 550°C facilitates co-precipitation of Cu-precipitates and M_2C (M = Mo, Cr, Fe) carbides

Secondary-hardening provided by M_2C carbides and slower coarsening of Cu-precipitates maintains a high yield-strength at 3 h of aging time, where impact toughness improves

NuCu-140

Mixture of ferritic lath and equiaxed ferrite microstructure in the as-quenched sample

Does not form M_2C carbides. Cu-precipitates coarsen faster than in HSLA-115

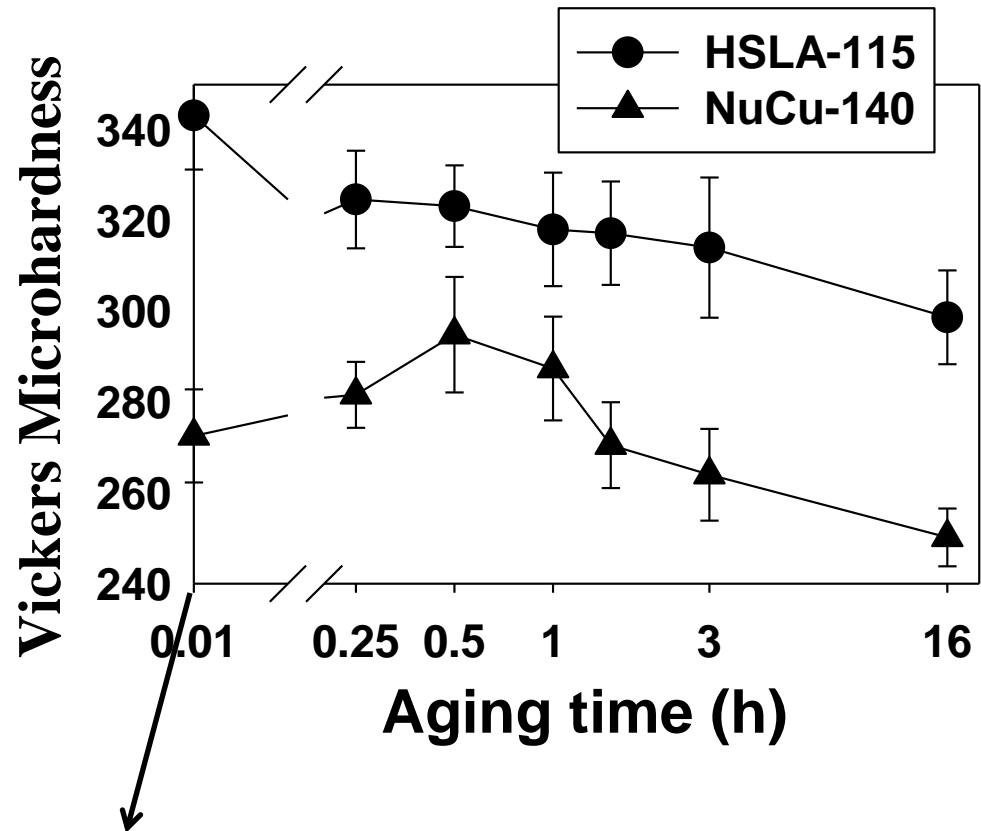
Significant decrease in strength at 3 h of aging time, where impact toughness improves

Chemical compositions

Element s (wt. %)	HSLA -115	NuCu- 140
C	0.05	0.05
Cu	1.29	1.64
Ni	3.37	2.77
Al	0.02	0.59
Mn	0.97	0.48
Si	0.22	0.50
Nb	0.02	0.065
<u>Cr</u>	<u>0.69</u>	<u>0.02</u>
<u>Mo</u>	<u>0.33</u>	-

Maintenance of high strength at long aging times in HSLA-115

- After aging for 3 h, microhardness decreases by 3.3% from its peak aged condition (1/4 h) in HSLA-115, while the decrease is 10.5% for NuCu-140 from its peak aged condition (0.5 h aging)
- This is due to a combination of secondary-hardening provided by the M_2C precipitates in HSLA-115 and slower coarsening kinetics of Cu precipitates in HSLA-115.



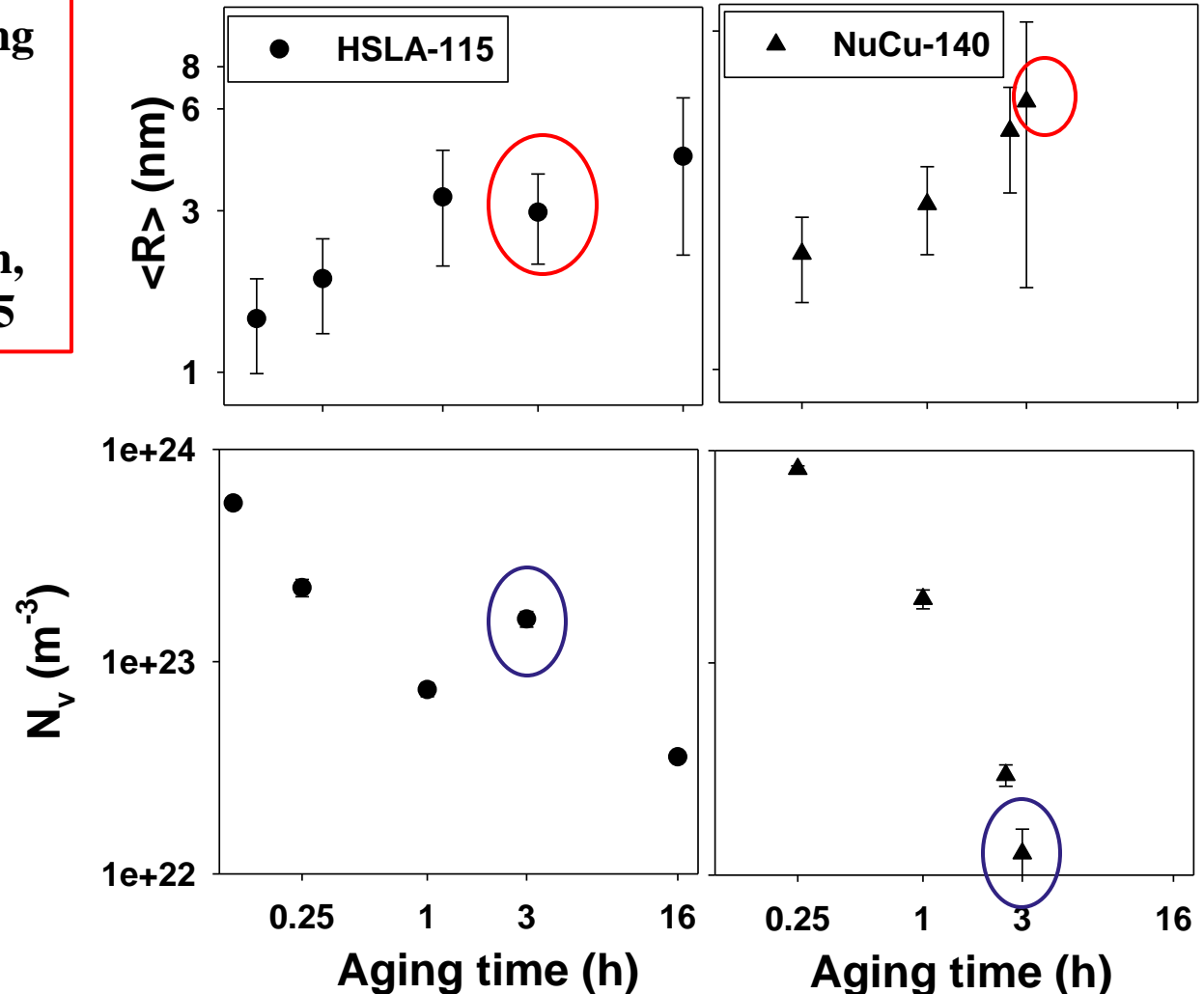
Slower coarsening of Cu-precipitates in HSLA-115 than in NuCu-140

• $\langle R(t) \rangle$ after 2.5 h of aging in NuCu140 is > 5 nm

• $\langle R(t) \rangle$ at 3 and 16 h of aging is 2.97 and 4.35 nm, respectively, in HSLA-115

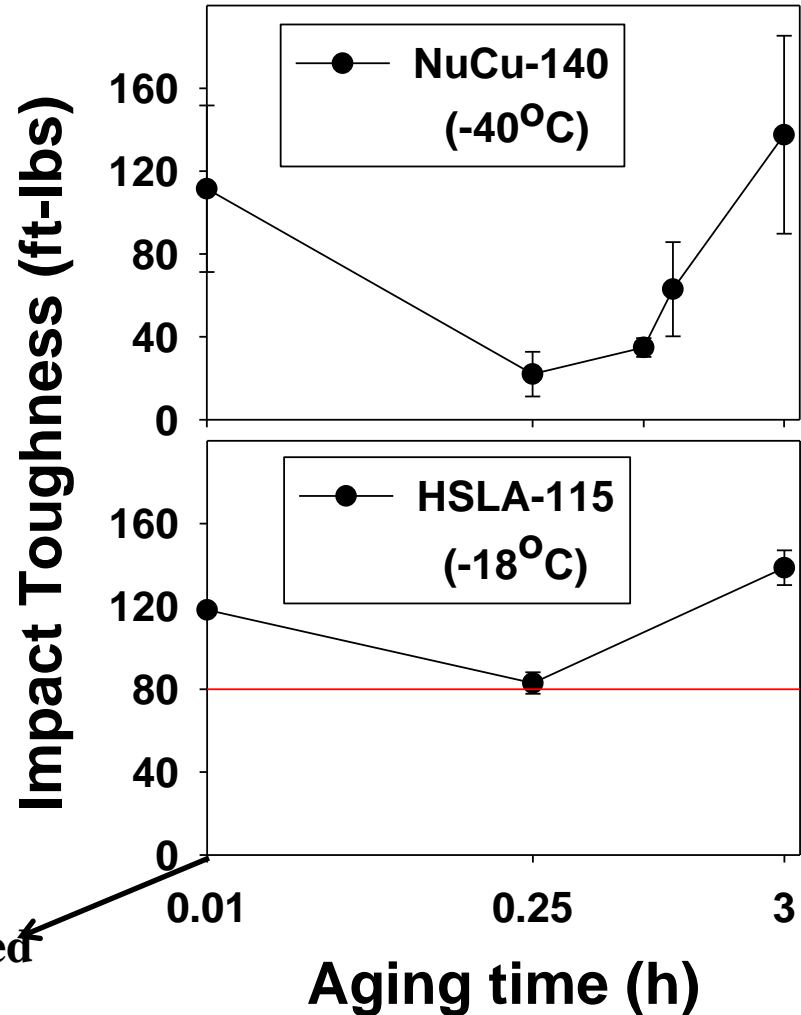
• N_v after 3 h of aging is one order of magnitude greater in HSLA-115 than in NuCu-140.

• Even after 16 h of aging, $N_v(t)$ in HSLA-115 is more than twice as large as in NuCu-140 at 3 h.



Similar trend of sub-ambient impact toughness in both steels

- Impact toughness decreases in both steels at 0.25 h from its solutionized and as-quenched value
- Impact toughness then increases to attain its maximum value at 3 h of aging in both steels
- Maintenance of high-strength at 3 h of aging in HSLA-115 is thus highly beneficial as it leads to a better combination of strength-impact toughness properties as compared to NuCu-140



as- quenched solutionized

80 ft-lbs is the minimum impact toughness requirement of these steels for Naval applications at -18°C

Conclusions from the aging study of HSLA-115 at 550°C

- **Strength achieved at 550°C aging temperature is significantly greater than required by U.S. Naval specifications, and thus HSLA-115 with its current composition is a candidate for higher-strength applications.**
- **Bulk mechanical properties obtained for HSLA-115 and NuCu-140 are compared and correlated with microstructural and sub-nanoscale observations using 3-D atom-probe tomography**
- **A tempering temperature of 550°C facilitates co-precipitation of Cu precipitates and M_2C carbides in HSLA-115. Cu precipitates appear to serve as nucleating agents for M_2C nucleation because M_2C carbides are co-located on Cu precipitates.**
- **Kinetics of Cu-precipitation is also affected by the co-located M_2C carbides, which may inhibit Cu-diffusion resulting in the deceleration of the coarsening of Cu-precipitates in HSLA-115. Similar phenomena were also observed in BA-160 steels.¹**
- **Unlike NuCu140, HSLA-115 tempered at 550°C, maintains its strength for long aging times. This result is significant as the desired toughness values are often obtained after significant tempering, which results in a loss of strength**

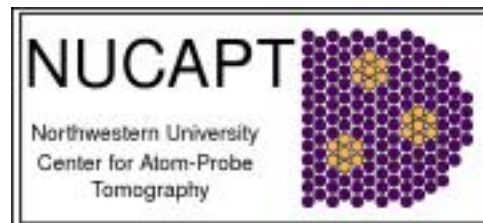
1. Mulholland, M. D., & Seidman, D. N. (2011). Nanoscale co-precipitation and mechanical properties of a high-strength low-carbon steel. *Acta Materialia*, 59(5), 1881-1897.

Acknowledgements

- **This research is supported by the Office of Naval Research. Dr. William M. Mullins, grant monitor.**
- **Atom-probe tomographic measurements were performed in the Northwestern University Center for Atom-Probe Tomography (NUCAPT). The 3-D atom-probe tomograph was purchased and upgraded with funding from NSF-MRI and ONR-DURIP programs. We also received funding from the Institute for Energy and Sustainability (ISEN) at Northwestern. Dr. Dieter Isheim is thanked for his kind help.**



NORTHWESTERN
UNIVERSITY

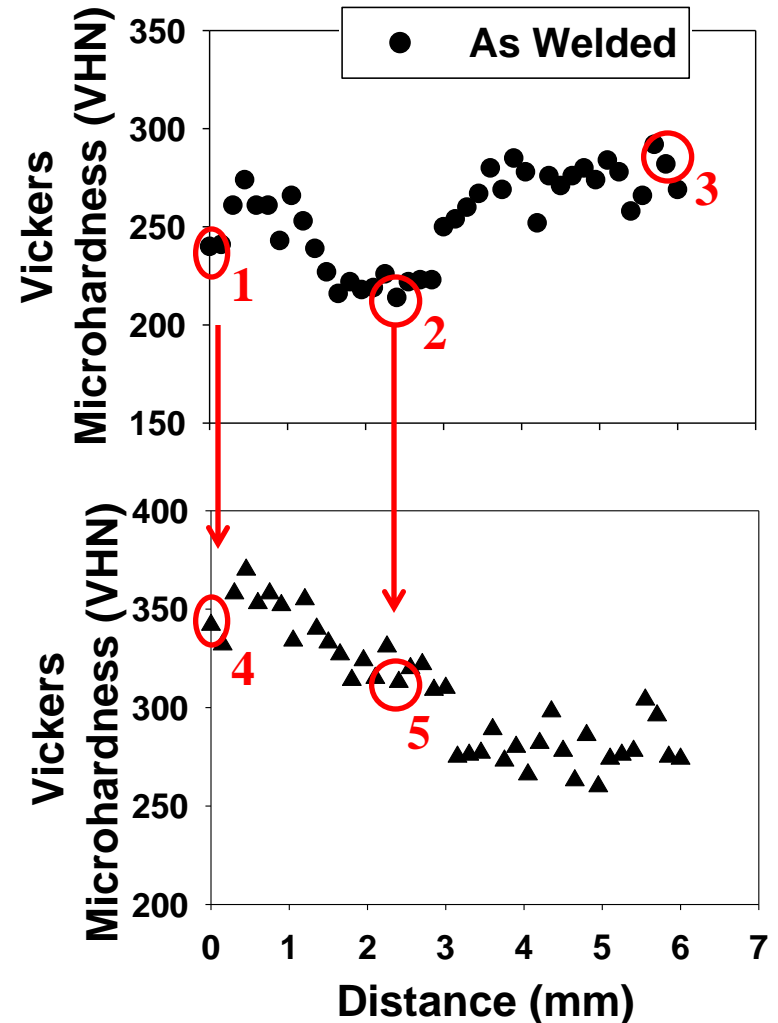


Welding Studies of NuCu-140 steels: Motivation

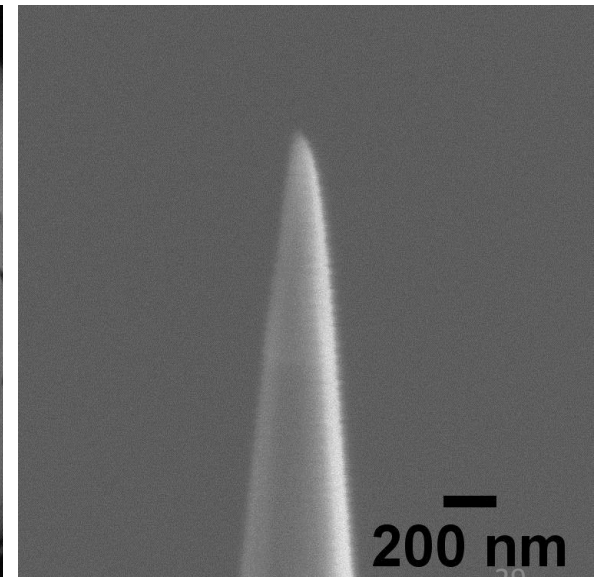
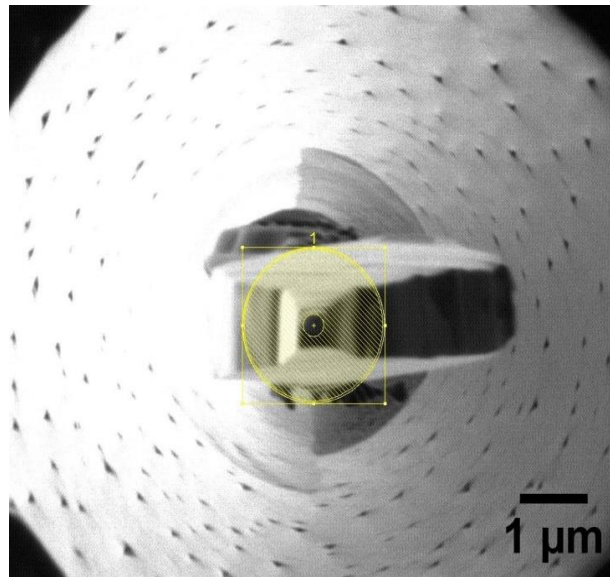
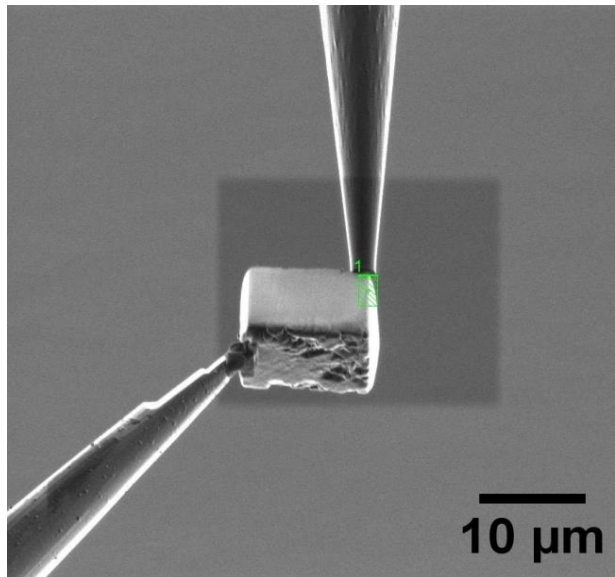
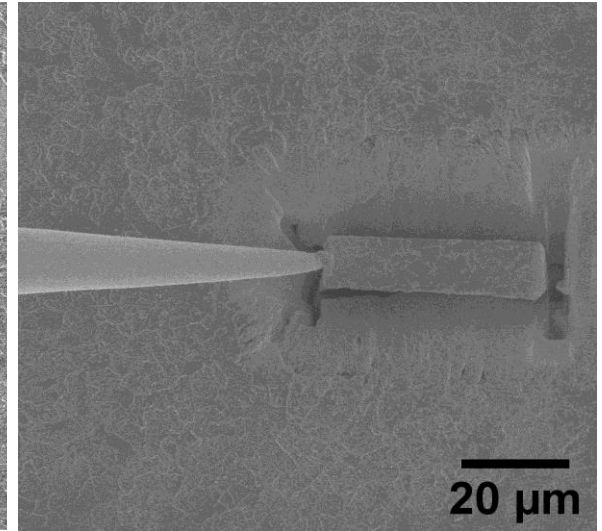
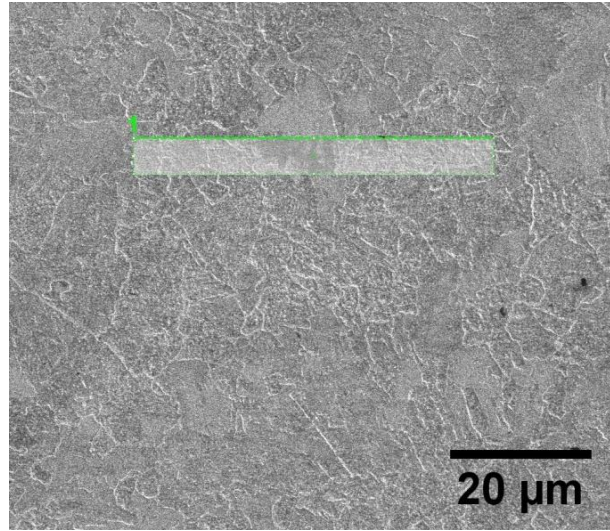
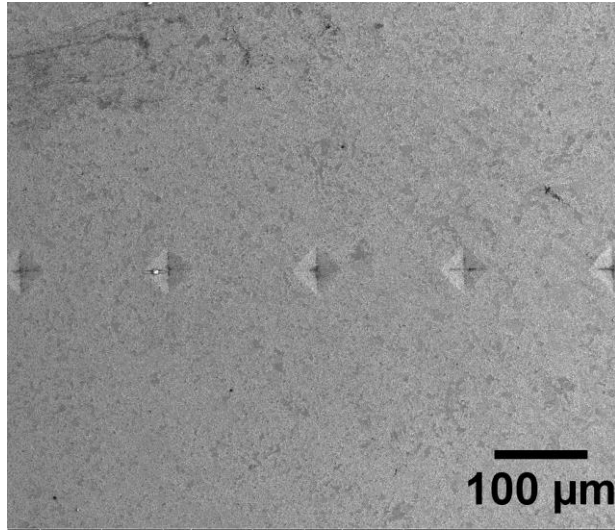
- **Welding of plate steels is the primary method of fabrication used by the U.S Navy for ship-construction.**
- **Large temperature gradients during the welding processes result in complex phase transformations and varied microstructures within a small volume of material**
- **High processing costs are a result of preheat and post-heat treatments, and inspection requirements during welding.**
- **There is, therefore, a need to understand the evolution of Cu-precipitates in the microstructures obtained after welding.**

Strength decrease in the fusion zone (1) and heat-affected (2) of the weldment

- Microhardness decrease in the fusion zone (1) and heat-affected zone (2) of the as-welded sample is recovered by a simple direct-aging treatment without affecting the hardness in the base-metal region, BM (3).
- This can be understood by studying the evolution of Cu-precipitates in these zones using 3-D atom-probe tomography
- Site-specific samples for 3-D atom-probe tomography examination are prepared using a dual-beam focused-ion beam microscope.



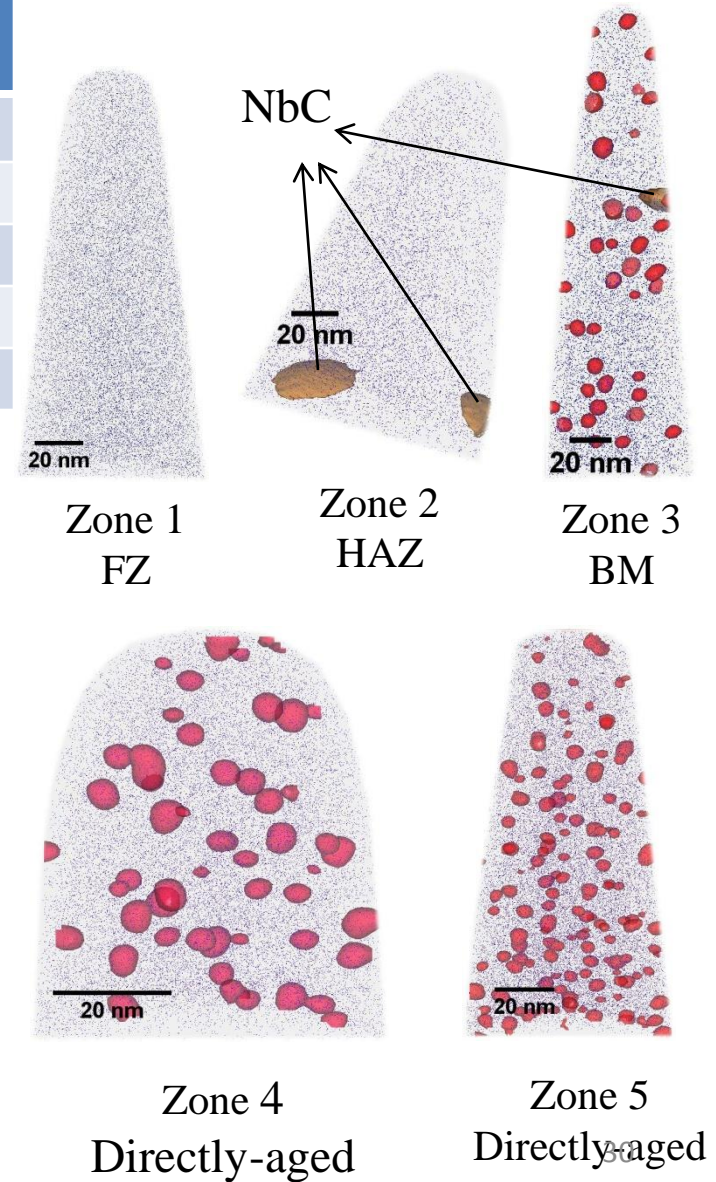
Site-specific 3-D atom-probe microtip preparation using dual-beam FIB microscope



3-D atom-probe tomographic results and conclusions

Zone	$\langle R \rangle$ (nm)	N_v (m^{-3})	V_f %
Zone1_aswelded	<u>No Cu precipitates observed</u>		
Zone2_aswelded	<u>No Cu precipitates observed</u>		
BM_aswelded	3.54 ± 1.05	$(9.35 \pm 1.44)E+22$	2.16 ± 0.33
Zone 4_aged	2.39 ± 0.75	$(3.75 \pm 0.34)E+23$	2.60 ± 0.24
Zone 5_aged	2.38 ± 0.68	$(4.11 \pm 0.15)E+23$	2.83 ± 0.10

- N_v of Cu-precipitates in zones 4 and 5 of the directly aged sample is greater and $\langle R \rangle$ is smaller than in the base metal (BM) of the as-welded sample
- This implies that decrease in microhardness in fusion zone (Zone 1) and heat-affected zone (Zone 2) of the as-welded sample is primarily due to the dissolution of the Cu-precipitates and not due to their over-aging in these zones
- An economically efficient direct-aging treatment, without a prior solutionizing step, is, therefore, sufficient to recover the loss in strength



Acknowledgements

- This research is supported by the Office of Naval Research. Dr. William M. Mullins, grant monitor.
- Atom-probe tomographic measurements were performed in the Northwestern University Center for Atom-Probe Tomography (NUCAPT). The 3-D atom-probe tomograph was purchased and upgraded with funding from NSF-MRI and ONR-DURIP. We also received funding from the Institute for Energy and Sustainability (ISEN) at Northwestern. Dr. Dieter Isheim is thanked for his kind help.



NORTHWESTERN
UNIVERSITY

